Journal of proteome research

Technical Note

pubs.acs.org/jpr

Evaluation of Parameters for Confident Phosphorylation Site Localization Using an Orbitrap Fusion Tribrid Mass Spectrometer

Samantha Ferries,[†,‡] Simon Perkins,[§] Philip J. Brownridge,[†] Amy Campbell,[†,‡] Patrick A. Eyers,[‡] Andrew R. Jones,[§] and Claire E. Eyers*[,†,‡]

[†]Centre for Proteome Research and [‡]Department of Biochemistry, Institute of Integrative Biology, University of Liverpool, Crown Street, Liverpool L69 7ZB, United Kingdom

[§]Department of Functional and Comparative Genomics, Institute of Integrative Biology, University of Liverpool, Crown Street, Liverpool L69 7ZB, United Kingdom

Supporting Information

ABSTRACT: Confident identification of sites of protein phosphorylation by mass spectrometry (MS) is essential to advance understanding of phosphorylation-mediated signaling events. However, the development of novel instrumentation requires that methods for MS data acquisition and its interrogation be evaluated and optimized for high-throughput phosphoproteomics. Here we compare and contrast eight MS acquisition methods on the novel tribrid Orbitrap Fusion MS platform using both a synthetic phosphopeptide library and a complex phosphopeptide-enriched cell lysate. In addition to evaluating multiple fragmentation regimes (HCD, EThcD, and neutral-loss-triggered ET(ca/hc)D) and analyzers for MS/MS (orbitrap (OT) versus ion trap (IT)), we also compare two commonly used bioinformatics platforms, Andromeda with PTM-score, and MASCOT with *ptmRS* for confident phosphopeptide identification and, crucially, phosphosite localization. Our findings demonstrate that optimal phosphosite identification is achieved using HCD fragmentation and high-resolution orbitrap-based MS/MS analysis, employing MASCOT/*ptmRS* for data interrogation. Although EThcD is optimal for confident site localization for a given PSM, the increased duty cycle compared with HCD compromises the numbers of phosphosites identified. Finally, our data highlight that a charge-state-dependent fragmentation regime and a multiple algorithm search strategy are likely to be of benefit for confident large-scale phosphosite localization.

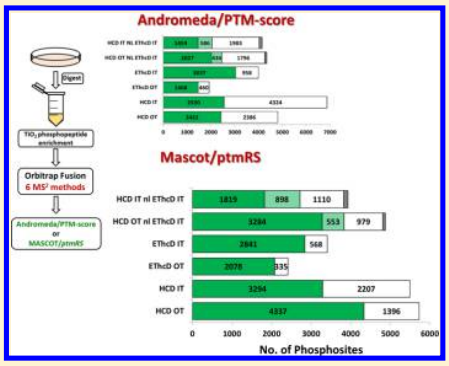

KEYWORDS: *mass spectrometry, phosphoproteomics, phosphosite localization, phosphorylation site, Orbitrap Fusion, ptmRS, PTM-score, MASCOT, Andromeda, EThcD*

INTRODUCTION

Protein phosphorylation is an essential, rapidly reversible, post-translational modification (PTM) with critical roles in nearly all biological processes. Defining these dynamic phosphorylation events is key to understanding their functional significance and gaining insight into the complex biology that they regulate. The ability to comprehensively and confidently decipher the phosphoproteome, the entire cellular phosphorylation state under a given set of conditions, thus yields indispensable information. Significant advances in mass spectrometry (MS) over the past decade have allowed for in-depth, although arguably incomplete, analysis of phosphoproteomes in a wide variety of complex biological systems.[1−12] The continual development of more sophisticated ways of generating and analyzing MS data is undoubtedly aiding phosphopeptide identification. However, from a mechanistic biological perspective, it is insufficient to have confidence in phosphopeptide identity if there is ambiguity regarding the site of modification within that peptide; consequently, it is of equal importance to define confidence in both phosphopeptide sequence and site of modification. Reviewers and users of such data generally understand this importance, and publication guidelines now typically require researchers to assess site localization confidence.[13]

MS-based analysis of (phospho)peptides relies on the acquisition of tandem MS (MS/MS) data from phosphopeptide-enriched samples, typically following proteolysis of complex cell extracts with proteases such as trypsin or LysC. The complexity and rapid regulation of the phosphoproteome means that significant numbers of samples often need to be analyzed. Maximizing the acquisition of information rich MS/MS data and its optimal interrogation to derive confident sequence information is essential for both phosphopeptide and phosphosite identity. In particular, confident phosphosite localization is critical if this key underpinning technology is to be of optimal benefit for the advancement of bioscience and interrogation of cell-signaling mechanisms. High-throughput

Received: May 28, 2017
Published: July 25, 2017

DOI: 10.1021/acs.jproteome.7b00337
J. Proteome Res. 2017, 16, 3448−3459

phosphoproteomics studies are currently suboptimal, with a recent isobaric labeling study demonstrating that only ~30% of phosphopeptides in an enriched complex mixture could be identified using conventional ion trap collision-induced dissociation (CID).[14] The efficiency of (phospho)peptide identification can undoubtedly be improved by using high-resolution mass analyzers for tandem MS. Additionally, confidence in phosphopeptide and phosphosite characterization can be enhanced by increasing the number of site-determining product ions, which we and others have shown can be aided by the exploitation of multiple complementary fragmentation modes.[15−20] The recent development of novel types of tribrid mass spectrometer, the Orbitrap Fusion series of instruments, which combine three mass analyzers (quadrupole, ion trap, orbitrap), is potentially of significant utility for such studies. The benefit of being able to perform both high- and low-energy collision-induced dissociation (HCD and CID, respectively) as well as electron-transfer dissociation (ETD), with product ion analysis being performed in either the ion trap or the orbitrap,[21−23] means that these instruments should be of great benefit in the quest for improved phosphoproteome analysis and unambiguous phosphosite identification. Although collisional dissociation is frequently implemented in proteomics workflows, there are limitations when used in phosphoproteomics pipelines due to preferential cleavage of the phosphoester bond. Such MS/MS spectra exhibit predominant neutral loss of phosphoric acid/phosphate (Δ98/Δ80) from the phosphorylated precursor ion and few informative product ions. Not only does this neutral loss impede peptide identification but also, once lost, it is often difficult to pinpoint the original site of modification. HCD[24] can overcome limited peptide backbone fragmentation, as the elevated energy applied and the additional kinetic energy of the ions means that they undergo further collisions, leading to richer, more informative, fragment ion spectra.[24−26] However, neutral loss at the expense of peptide backbone fragmentation can still arise with an HCD fragmentation regime,[26] compromising confident phosphosite localization. In contrast, the nature of phosphopeptide ion fragmentation by ETD means that the phosphate group is retained on the modified residue, often allowing the site of modification to be identified with greater confidence. Application of ETD has typically been limited for large-scale studies, in part due to its availability only on selected MS platforms but also due to inherent limitations. ETD requires longer reaction times, and fragmentation is generally much less efficient than collision-mediated dissociation, in particular, for low charge states (where $z = 2$). The development of EThcD,[18] a dual fragmentation strategy that combines ETD and HCD resulting in MS/MS spectra containing b/y and c/z ions, is reported to enhance localization of various PTMs on peptides and proteins, including phosphorylation.[19,27−29]

The number of potential phosphopeptide MS acquisition strategies, particularly with the new generation of versatile tribrid Orbitrap instruments, means that it can be extremely complicated and time-consuming to establish an "optimal" phosphoproteomics pipeline. There are numerous challenges associated with optimizing instrument settings to maximize phosphopeptide identification and, crucially, confident site localization. The added capability of the Orbitrap Fusion instruments to parallelize acquisition of MS^1 in the high-resolution orbitrap, while acquiring, at a faster rate, lower resolution MS^2 in the ion trap (if required), means that there can be significant advantages for high-throughput proteomics using this type of tribrid instrument. The number of possible strategies for MS(/MS) data acquisition (orbitrap versus ion trap) as well as potential fragmentation regimes (CID, HCD, ETcaD, EThcD, with or without neutral loss considerations that may be used for triggering additional MS^2/MS^3 acquisition or multistage acquisition (MSA)) means that the combinatorial options for MS data acquisition are vast.

Here we systematically evaluate eight acquisition modes on the tribrid Orbitrap Fusion MS platform using a library of synthetic phosphopeptide standards and a complex phosphopeptide-enriched cell lysate preparation. We define optimal MS acquisition settings for both phosphopeptide identification and phosphosite localization, interrogating these data sets using two commonly used phosphoproteomics bioinformatics platforms: Proteome Discoverer (PD) with MASCOT and phosphoRS (*ptmRS*) and MaxQuant with Andromeda and PTM score, comparing the benefits of each for confident peptide identification and phosphosite localization. We also evaluate the effect of charge state and the number of putative phosphorylatable residues on site localization confidence. Although previous experience had suggested that optimal phosphosite localization would require electron-transfer-mediated fragmentation, this was not observed for the vast majority of phosphopeptides.

We anticipate that these data, and the analysis thereof, will serve as an ideal starting point for laboratories worldwide looking to establish high-throughput phosphoproteomics using this next generation of tribrid MS instrumentation.

MATERIALS AND METHODS

Reagents

All chemicals were purchased from Sigma-Aldrich unless otherwise stated. The synthetic phosphopeptide library was purchased from Intavis.

Cell Culture and Lysis

U2OS T-Rex Flp-in cells were maintained in DMEM supplemented with 10% (v/v) fetal bovine serum, penicillin (100 U/mL), streptomycin (100 U/mL), and L-glutamine (2 mM) at 37 °C, 5% CO_2. Once 80% confluence was reached, cells were washed with PBS and released with trypsin (0.05% (v/v)). Cells were centrifuged at 220*g* and lysed with 500 μL of 0.25% (w/v) RapiGest SF (Waters, U.K.) in 50 mM ammonium bicarbonate with 1× PhosSTOP phosphatase inhibitor cocktail tablet (Roche). The lysate was sonicated briefly and centrifuged at maximum speed for 20 min. Protein concentration was determined using the Bradford assay and 4 mg was set aside for protein digestion.

Sample Preparation

Disulfide bonds were reduced by the addition of 3 mM DTT in 50 mM ammonium bicarbonate and heated to 60 °C for 15 min. The resulting free cysteine residues were alkylated with 14 mM iodoacetamide (dark, room temperature, 45 min) and excess iodoacetamide quenched by the addition of DTT to a final concentration of 7 mM. Proteins were digested overnight with trypsin (2% (w/w); Promega) at 37 °C. RapiGest SF hydrolysis was induced by the addition of trifluoroacetic acid (TFA) to 1% (v/v) and incubated at 37 °C for up to 2 h, 400 rpm. Insoluble hydrolysis product was removed by centrifugation (13 000*g*, 15 min, 4 °C).[15] Peptides were desalted using C18 macro columns (Harvard Apparatus, Cambridge, U.K.). In brief, columns were conditioned with 100% methanol and

DOI: 10.1021/acs.jproteome.7b00337
J. Proteome Res. 2017, 16, 3448−3459

washed with H_2O and 1% (v/v) TFA. Peptides were loaded on to the column and centrifuged for 1 min at 110*g*. The flow-through was reapplied a total of five times, and peptides were eluted with 80% (v/v) MeCN and 1% (v/v) TFA and dried to completion by vacuum centrifugation.

Dried peptides were dissolved in loading buffer (80% (v/v) MeCN, 5% (v/v) TFA, 1 M glycolic acid), sonicated, and incubated with 5 mg titanium dioxide resin (5:1 (w/w) beads/protein; GL Sciences) at 1400 rpm for 10 min on a thermomixer. Wash steps were performed sequentially with 150 μL of loading buffer, 150 μL of wash buffer 1 (80% (v/v) MeCN, 1% (v/v) TFA), and 150 μL of wash buffer 2 (10% (v/v) MeCN, 0.2% (v/v) TFA). Phosphopeptides were eluted with increasing pH (1% (v/v) ammonium hydroxide and 5% (v/v) ammonium hydroxide) and dried to completion by vacuum centrifugation.[9] Peptides were resolubilized in 240 μL of 96% (v/v) H_2O, 3% (v/v) MeCN, 1% (v/v) TFA.

Liquid Chromatography–Mass Spectrometry

Reversed-phase capillary HPLC separations were performed using an UltiMate 3000 nano system (Dionex) coupled in-line with a Thermo Orbitrap Fusion tribrid mass spectrometer (Thermo Scientific, Bremen, Germany). Synthetic phosphopeptide standards (~10 pmol, split into five pools to separate phosphoisomers and thus ensure confidence in phosphosite localization) and 6 μL of enriched phosphopeptides (equivalent to 100 μg of digested cell lysate) were loaded onto the trapping column (PepMap100, C18, 300 μm × 5 mm), using partial loop injection, for 7 min at a flow rate of 9 μL/min with 2% (v/v) MeCN, 0.1% (v/v) TFA and then resolved on an analytical column (Easy-Spray C18 75 μm × 500 mm, 2 μm bead diameter column) using a gradient of 96.2% A (0.1% (v/v) formic acid (FA)): 3.8% B (80% (v/v) MeCN, 0.1% (v/v) FA) to 50% B over 97 min at a flow rate of 300 nL/min.

MS(/MS) data were acquired on an Orbitrap Fusion as follows: All MS^1 spectra were acquired over m/z 350–2000 in the orbitrap (120 K resolution at 200 m/z for high–low strategies and 60K resolution at 200 m/z for high–high strategies); automatic gain control (AGC) was set to accumulate 2×10^5 ions, with a maximum injection time of 50 ms. Data-dependent tandem MS analysis was performed using a top-speed approach (cycle time of 3 s) with multiple fragmentation methods tested (see Table 1 for summary of parameters). The normalized collision energy was optimized at 32% for HCD. MS^2 spectra were acquired with a fixed first m/z of 100. The intensity threshold for fragmentation was set to 50 000 for orbitrap methods and 5000 for ion trap methods and included charge states 2+ to 5+. A dynamic exclusion of 60 s was applied with a mass tolerance of 10 ppm. For neutral-loss-triggered ETcaD/EThcD methods, fragmentation was enabled for all precursor ions exhibiting neutral loss of mass 97.9763 or 80 Da with a mass tolerance of 20 ppm for orbitrap data and 0.5 m/z for ion trap data, where the neutral loss ion was one of the top 10 most intense MS^2 ions. ETD calibrated parameters were applied. AGC was set to 10 000 with a maximum injection time set at 50 ms for IT and 70 ms for OT; ETD reaction time was charge-dependent.

Table 1. MS Data Acquisition Methods Evaluated[a]

method	resolution (MS^1)	mass analyzer (MS^2)	resolution (MS^2)
HCD OT	60K	orbitrap	30K
HCD IT	120K	ion trap	rapid
EThcD OT	60K	orbitrap	30K
EThcD IT	120K	ion trap	rapid
HCD OT nl EThcD IT	60K	orbitrap	30K/rapid
HCD OT nl ETcaD IT	60K	orbitrap	30K/rapid
HCD IT nl EThcD IT	120K	ion trap	rapid
HCD IT nl ETcaD IT	120K	ion trap	rapid

[a]IT: ion trap; OT: orbitrap; nl: neutral loss. See Supplementary Table 1 for full details of MS data acquisition parameters. All MS^1 analysis was performed in the orbitrap.

Data Analysis

Data were processed using either Thermo Proteome Discoverer (v. 1.4) in conjunction with MASCOT (v 2.6) or with Andromeda integrated in MaxQuant (1.5.8.0) using default settings unless otherwise specified. To address the requirement of MASCOT for centroided data, raw data files were converted to mzML format to perform MS^2 deisotoping prior to processing with MASCOT through the PD pipeline. Peak lists were searched against a database containing either the synthetic phosphopeptide sequences or the human UniProt database (201512; 20 187 sequences). Parameters were set as follows: MS^1 tolerance of 10 ppm; MS^2 mass tolerance of 0.01 Da for orbitrap detection, 0.6 Da for ion trap detection; enzyme specificity was set as trypsin with two missed cleavages allowed; no enzyme was defined for the phosphopeptide library processing; carbamidomethylation of cysteine was set as a fixed modification; and phosphorylation of serine, threonine, and tyrosine and oxidation of methionine were set as variable modifications. Nonfragment filtering was applied to ETD scans to remove the precursor peak within a 4 Da window and remove charge reduced precursor and neutral loss ions from charge reduced precursor ions within a 2 Da window. *ptm*RS was run in PhosphoRS mode using diagnostic fragment ions and analyzer-specific fragment ion tolerances, as previously defined in the search. For EThcD data, "Treat all spectra as EThcD" option was set to "True". Data were filtered to a 1% false discovery rate (FDR) on PSMs using automatic decoy searching with MASCOT and a target-decoy search with Andromeda.

RESULTS AND DISCUSSION

Comparison of Fragmentation Methods and MS^2 Resolution Settings for Identification and Site Localization of Phosphopeptide Standards

To evaluate the advanced capabilities of the Orbitrap Fusion tribrid mass spectrometer for site-specific phosphopeptide identification, we designed a series of MS acquisition methods to assess the benefits of using either the high-resolution orbitrap or the lower resolution ion trap mass analyzers. In the first instance we analyzed a commercially available synthetic library of phosphopeptides[30] that comprised tryptic peptides previously observed in multiple large-scale phosphopeptide studies. The library was designed such that the typical composition and length observed in bottom-up proteomics is represented, with a natural occurrence of unmodified and phosphorylated serine, threonine, and tyrosine residues.

In addition to differing in resolving power, there are significant differences in speed and sensitivity between the orbitrap (OT) and ion trap (IT) mass analyzers. HCD, EThCD, and neutral-loss (NL)-triggered ETD-mediated fragmentation strategies, where ions exhibiting precursor neutral loss of 98 amu (arising due to the characteristic loss

DOI: 10.1021/acs.jproteome.7b00337
J. Proteome Res. 2017, 16, 3448–3459

Table 2. MS Acquisition and Data Analysis Methods Evaluated Using Synthetic Phosphopeptides[a]

search engine		HCD OT	HCD IT	EThcD OT	EThcD IT	HCD OT nl EThcD	HCD OT nl ETcaD	HCD IT nl EThcD	HCD IT nl ETcaD
Andromeda	no. PSM[b]	705 ± 4	984 ± 16	407 ± 18	515 ± 88	625 ± 194	650 ± 30	838 ± 37	745 ± 36
	no. unique phosphopeptides	154	159	146	152	156	154	154	155
	no. phosphosites	168	173	160	166	170	168	168	170
	no. phosphosites correctly localized with PTM-score	155	150	155	156	152	154	147	150
	% phosphosites correctly localized with PTM-score	92%	87%	97%	94%	89%	92%	88%	88%
MASCOT	no. PSM[b]	889 ± 1	1497 ± 11	417 ± 1	654 ± 52	866 ± 107	868 ± 13	1029 ± 30	940 ± 29
	no. unique phosphopeptides	164	168	149	156	162	160	159	157
	no. phosphosites	179	183	163	165	180	175	173	171
	no. phosphosites correctly localized with *ptm*RS	172	151	154	151	167	163	154	144
	% phosphosites correctly localized with *ptm*RS	96%	83%	94%	92%	93%	93%	89%	84%

[a]For each of the eight orbitrap Fusion MS acquisition methods (Table 1, Table S1) the number of peptide spectrum matches (PSMs) is presented (n = two technical replicates), together with the number of unique peptides (out of a total of 175) and phosphosites (total 191) as well as the number and percentage of correctly localized phosphosites using either Andromeda with PTM-score (top) or MASCOT and ptmRS (bottom), according to the top-ranked PSM. [b]Mean values are presented ± SD.

of H_3PO_4 from phosphorylated peptide ions[16,17,31]) or 80 amu (arising due to loss of HPO_3) following HCD were also compared (Table 1; Table S1).

The phosphopeptide library, containing 175 unique phosphopeptides (191 phosphorylation sites), was divided into five pools for LC−MS/MS analysis. Isomeric phosphopeptides (where the same peptide sequence is modified on a different residue) were allocated to different analytical pools to ensure that site localization could be defined absolutely. The five pools of synthetic phosphopeptide standards were each analyzed in duplicate using the eight MS acquisition methods, assessing both phosphopeptide identification and phosphosite localization (Table 2, Figure S1).

As an extension of previously published studies[30,32] we also assessed the ability of two commonly used phosphoproteomics data analysis platforms, MASCOT integrated into PD using ptm*RS* (a slightly modified version of phosphoRS[33]) for phosphosite localization and Andromeda with MaxQuant and PTM-score,[34] to identify the synthetic phosphopeptides from all eight data sets (Table 2).

Implementation of either the Andromeda or MASCOT search algorithms resulted in notably fewer PSMs using EThcD compared with HCD, independent of whether MS^2 was performed in the orbitrap or the ion trap (Table 2). This result can be explained by the increase in duty cycle for this mixed mode fragmentation regime. Consequently, fewer phosphopeptides were identified with EThcD OT compared with the analogous HCD OT and likewise for EThcD IT compared with HCD IT (Table 2). However, the higher percentage of PSMs with correctly localized phosphosites following EThcD IT (94% compared with 87% for Andromeda/PTM-score; 92% compared with 83% for MASCOT/ptm*RS* for EThcD IT or HCD IT, respectively) translated to the same or higher numbers of correctly site localized phosphosites being characterized overall with EThcD IT than HCD IT (Table 2, Figure 1A, Figure S2). These findings are in agreement with previous observations on different instrument platforms, which highlight the benefit of mixed mode fragmentation for improved phosphosite localization.[19] For the high-resolution OT data, there was a notable difference in the performance of the two search engines. Consequently, while phosphosite localization confidence increased with EThcD compared with HCD (resulting in the same number of correctly localized phosphosites) using Andromeda/PTM-score, this was not the case with MASCOT/*ptmRS*. 172 phosphosites were correctly identified with HCD OT, whereas EThcD OT yielded only 154 correctly localized phosphosites. The benefits of high-resolution MS^2 acquisition therefore appear to outweigh the increased duty cycle associated with EThcD when using MASCOT/*ptmRS* for this phosphopeptide library.

When considering HCD fragmentation, with or without NL-triggered ET(hc/ca)D, phosphosite localization with both bioinformatics platforms was optimal (higher percentage) with high-resolution orbitrap MS^2 analysis, likely due to the improved confidence afforded by the enhanced mass accuracy as compared with low-resolution ion trap MS^2 measurements (Table 2, Figure 1A, Figure S1). Interestingly, Andromeda/PTM-score yielded fewer numbers overall, both of unique phosphopeptides and of correctly localized phosphosites, compared with MASCOT/*ptmRS*, irrespective of MS method. A maximum of 159 unique phosphopeptides (155 correctly localized phosphosites) were identified from the pool of 175 synthetic phosphopeptides with Andromeda/PTM-score compared with 168 phosphopeptides (172 correctly localized phosphosites) when the same data were interrogated using MASCOT/*ptmRS*.

With both search algorithms, HCD IT was optimal for both PSMs and the numbers of unique phosphopeptide identified, as might be expected given the possibility for parallelization of MS^1 data acquisition in the orbitrap and concurrent MS^2 analysis in the ion trap. However, site localization confidence, the critical parameter from the point of view of biological inference, was either optimal (*ptmRS*) or of equal performance (PTM-score) using the HCD OT method.

Upon further examination of the workflows exploiting neutral-loss-triggered ETcaD, the vast majority (89−93%) of correctly site-localized phosphopeptides were derived from the HCD spectra rather than the ETcaD spectra triggered following precursor neutral loss. The additional incorporation of ETcaD in this regime thus appeared to offer no benefit for either phosphopeptide identification or site localization over that achieved with HCD alone. Indeed, the number of PSMs was compromised due to the increase in duty cycle for the ETcaD

DOI: 10.1021/acs.jproteome.7b00337
J. Proteome Res. 2017, 16, 3448−3459

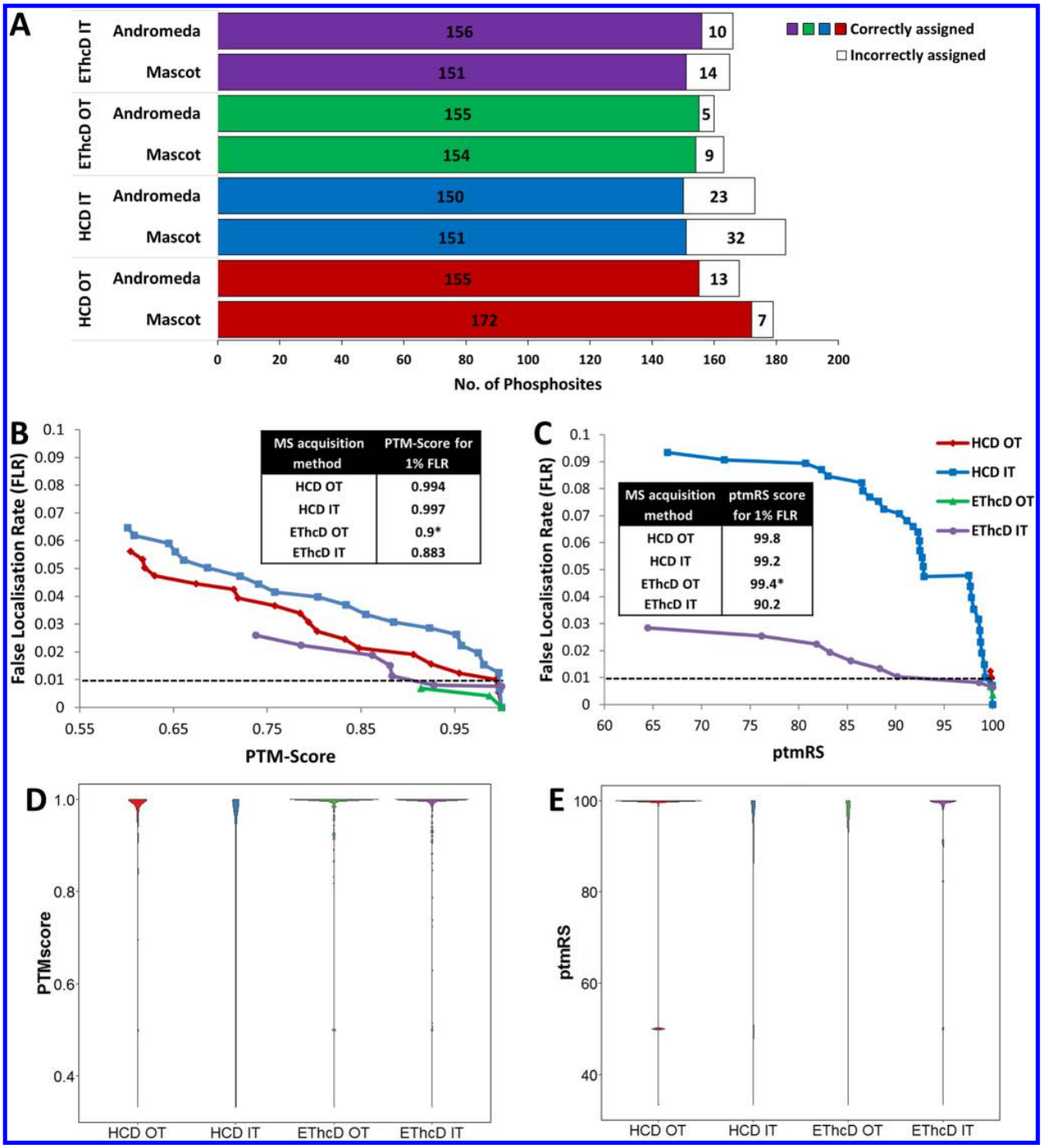

Figure 1. Fragmentation method-specific phosphosite localization. (A) Number of correctly assigned (HCD OT: red; HCD IT: blue; EThcD OT: green; EThcD IT: purple) and incorrectly assigned (white) phosphosites from the synthetic phosphopeptide library (Table 1; Table S1). (B,C) False localization rate (FLR) determination for the four different basic MS^2 acquisition strategies using either Andromeda/PTM-score (B) or MASCOT/ptmRS (C). Distributions of PTM-score (D) or ptmRS (E) for each of the four MS^2 methods. *Site localization scores equivalent to 0.7% FLR.

component of this method. The HCD IT/OT nl ETcaD IT methods are therefore not discussed in subsequent analytical comparisons.

A significant advantage of using synthetic phosphopeptides of known sequence is the ability to define false localization rates (FLRs) specific to the MS acquisition method employed by counting the numbers of correct and incorrectly site-localized PSMs[30] (Figure 1B–E). The distribution of site-localization scores for each of the four unique fragmentation modes, HCD OT, HCD IT, EThcD OT, EThcD IT, with each of the two informatics pipelines is presented in Figure 1. Akin to previous observations on different MS platforms with both synthetic phosphopeptides[30] and a complex phosphopeptide enriched cell lysate,[32] both site-localization tools require MS acquisition method specific scores to yield a 1% FLR (Figure 1B,C). It is of interest to note that although fewer phosphosites were

DOI: 10.1021/acs.jproteome.7b00337
J. Proteome Res. 2017, 16, 3448–3459

Table 3. MS Acquisition and Data Analysis Methods Evaluated Using Phosphopeptide Enriched Human Cell Lysate[a]

search engine		HCD OT	HCD IT	EThcD OT	EThcD IT	HCD OT nl EThcD	HCD IT nl EThcD
Andromeda/PTM-score	no. unique phospho PSMs	5414 ± 197	6396 ± 728	1947 ± 1	3321 ± 42	5452 ± 88	5506 ± 659
	no. unique phosphopeptides	4214	5632	1730	3315	3702	3494
	no. phosphosites	4808	6877	1928	3995	4345	4145
	no. phosphosites ≤1% FLR	2422 (50%)	2550 (37%)	1468 (76%)	3037 (76%)	2472 (57%)	2045 (49%)
MASCOT/*ptm*RS	no. unique phospho PSMs[b]	5118 ± 45	4705 ± 269	2084 ± 26	2847 ± 197	4966 ± 45	4297 ± 69
	no. unique phosphopeptides	4957	4920	2148	2947	4153	3398
	no. phosphosites	5733	5501	2413	3409	4880	3933
	no. phosphosites ≤1% FLR	4337 (76%)	3294 (60%)	2078 (86%)	2841 (83%)	3837 (79%)	2717 (69%)

[a]For each of the six Orbitrap Fusion MS acquisition methods (Table 1, Table S1) the number of peptide spectrum matches (PSMs) at 1% FDR is presented together with the total number of unique phosphopeptides and phosphosites using either Andromeda with PTM-score (top) or MASCOT and ptmRS (bottom). The number of phosphosites with an FLR ≤ 1% is also presented. [b]Mean values are ± SD, n = 2.

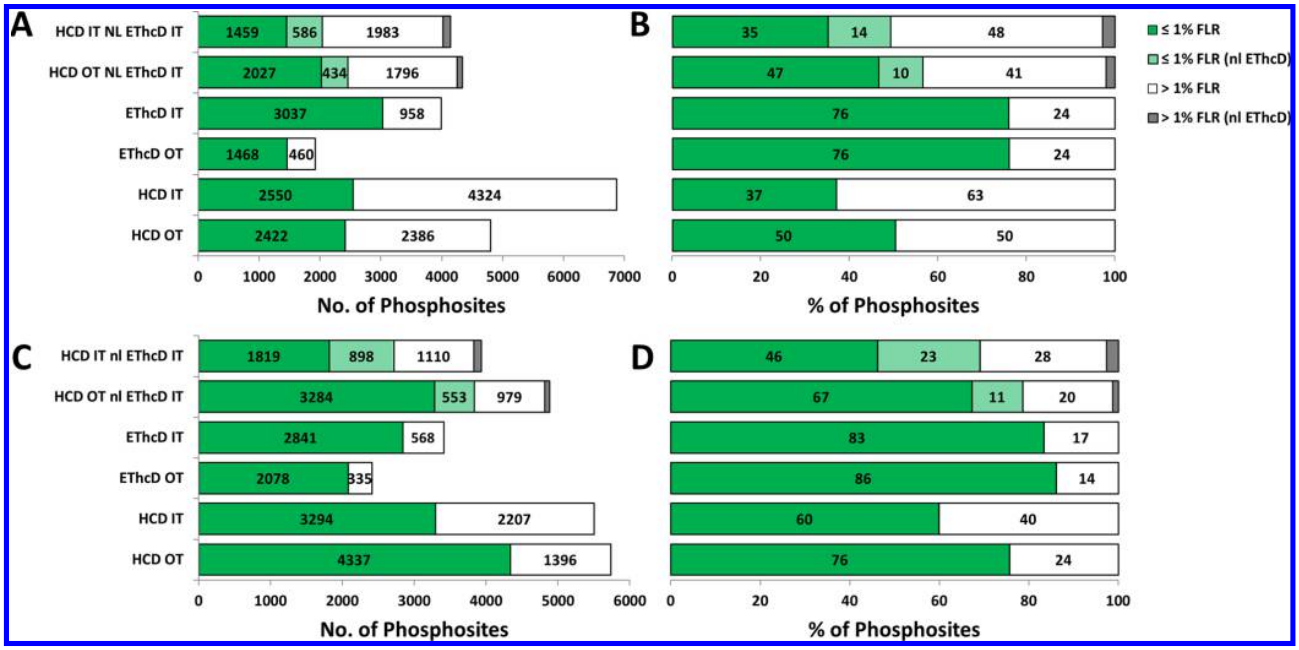

Figure 2. Comparison of method-dependent phosphorylation site localization. Confidently localized phosphorylation sites (FLR ≤ 1%, green) or ambiguous phosphosite assignments (white, gray) from a TiO_2-enriched U2OS cell lysate using either (A,B) Andromeda/PTM-score or (C,D) MASCOT/ptmRS for each of the six Orbitrap Fusion MS acquisition methods. Phosphosites assigned by virtue of neutral-loss (NL)-triggered EThcD are also presented. Number (A,C) or percentage (B,D) of phosphosites identified is indicated for each condition.

incorrectly localized overall with HCD OT compared with HCD IT with both search engines, this does not correlate with a lower site localization score. *ptmRS* exhibits a bimodal distribution for high-resolution MS^2 data, with clustering of values around *ptmRS* = 100 and *ptmRS* = 50, indicating either "certainty" or lack of discriminatory evidence between two possible sites, respectively. In contrast, PTM-score values are more evenly distributed (red plots in Figure 1D,E). This difference is likely due to how the two algorithms were developed; while phosphoRS was optimized with both high- and low-resolution data,[33] PTM-score was originally developed for phosphosite localization using low mass accuracy ion-trap generated CID data.[35] Unlike phosphoRS, PTM-score treats all observed MS^2 peaks as integer masses,[33,36] meaning that there is limited benefit using PTM-score when high-resolution data have been acquired. Furthermore, while PTM-score searches the "n" most intense peaks within a bin of 100 m/z to identify site-determining product ions, *ptmRS* considers the total number of extracted peaks across the full mass range of the MS^2 spectrum, overcoming potential issues of uneven peak distribution in individual m/z bins,[33,36] and is thus better suited for data generated with high-resolution mass analyzers.

Both localization tools underestimated the true FLR for EThcD IT data (Figure 1B,C), demonstrating the additional benefit of generating site determining c/z as well as b/y ions within a single spectrum. A 1% FLR could not be computed for the EThcD OT data set because insufficient incorrectly localized phosphopeptides were identified from the library. Instead, the scores defined for this fragmentation mode (PTM-Score = 0.9; *ptmRS* = 99.4, Figure 1B,C) represent an FLR of 0.7%. The other PTM-score and *ptmRS* values computed for phosphosite localization at a 1% FLR are broadly in agreement with those previously defined for a larger synthetic phosphopeptide library using a different orbitrap-based MS platform, demonstrating that the MS acquisition methods and

DOI: 10.1021/acs.jproteome.7b00337
J. Proteome Res. 2017, 16, 3448−3459

the associated bioinformatics platforms are largely transferable between similar platforms.[30]

In addition to the 1% FDR filtering, "default settings" in Andromeda apply a score cut off of 40 for post-translationally modified peptides. To investigate whether this artificially reduced the numbers of phosphopeptides identified from our library, all eight data sets were searched again with Andromeda, having removed the requirement for scores to exceed 40 (Table S2). An analogous threshold for comparison with MASCOT could not be set because there is not a perfect linear relationship between the two scoring algorithms.[35] Upon removal of this score filter in Andromeda, the numbers of confidently identified phosphorylation sites were broadly similar, with the exception of the high-resolution HCD OT and HCD OT nl EThcD data sets, where an additional seven and six phosphosites were identified, respectively. The resultant minimal change in confidently assigned phosphosites (max. 4% with HCD OT; 2% decrease with EThcD IT) meant that amendment of the default settings in Andromeda did not warrant further investigation. Default settings for both search engines were thus used in subsequent investigations, with these also being the parameters that most end-users will typically apply.

Phosphopeptide Identification from a Phosphopeptide Enriched Complex Human Cell Lysate

Having evaluated the eight MS acquisition methods using the phosphopeptide library, we were able to define six methods for this tribrid MS platform worthy of further investigation based on the numbers of correctly site-localized phosphopeptides. Performance of these six MS acquisition strategies for phosphopeptide identification and phosphosite localization was then evaluated using a larger data set derived from a more complex, biologically relevant sample. Phosphopeptides were enriched from a U2OS cell lysate using TiO_2, and aliquots (6 μL, equivalent to 100 μg from 4 mg digested cell lysate) of the same phosphopeptide-enriched sample were analyzed in duplicate by LC−MS/MS using HCD OT, HCD IT, EThcD OT, EThcD IT, HCD OT nl EThcD IT, or HCD IT nl EThcD IT (Table S1).

The number and overlap of unique phosphopeptide identifications using either Andromeda/PTM-score or MASCOT/*ptmRS* is presented for each of the MS acquisition methods (Table 3, Figure 2, Figures S2 and S3). Of the six methods assessed, HCD IT exhibited the least overlap between technical replicates, with up to 44% of phosphopeptides being unique to a single LC−MS/MS run. Other methods exhibited between ∼20% (HCD OT nl EThcD IT) and 25% (HCD OT) overlap (Figure S1).

The highest total number of unique phosphopeptides from the enriched U2OS cell lysate (6877 phosphopeptides above a 1% FDR) was identified using HCD IT and Andromeda (Table 3, Figure 2, Figures S4−S6). This regime maximizes on the capability of the Orbitrap Fusion to parallelize high-resolution MS^1 acquisition in the orbitrap while simultaneously acquiring MS^2 data in the ion trap. Interestingly, there was little difference in the number of unique phosphopeptides identified using MASCOT when MS^2 was performed in the OT versus the IT; 4957 phosphopeptides were confidently identified for HCD OT compared with 4920 phosphopeptides using HCD IT (Table 3). This is almost certainly due to the enhanced confidence in phosphopeptide identification that results when MS data are acquired with higher mass accuracy, as is the case with HCD OT; however, it is particularly interesting to note how Andromeda and MASCOT differentially handle high-resolution and low-resolution MS^2 data (discussed in more detail below).

An important reason for undertaking this study was to evaluate confidence in phosphosite localization. Under the conditions examined, phosphosite localization was optimal when utilizing HCD OT and MASCOT/*ptmRS* searching. Of the 5733 phosphosites identified, 76% (4337) were confidently site localized under these conditions (Table 3, Figure 2, Figures S4−S6). For the same data set, 4808 phosphosites were defined using Andromeda/PTM-score, of which 50% failed to meet the 1% FLR cutoff for confident site localization using the previously defined PTM-score of 0.994. Although the proportion of confidently site localized phosphopeptides is optimal overall with the EThcD regimes (both OT and IT), as we observed with the phosphopeptide library data set, the number of phosphosites was compromised compared with either the equivalent HCD method or the neutral-loss driven strategies. Even considering that the site localization scores applied to the EThcD OT data was slightly more conservative (equating to 0.7% FLR, rather than 1% FLR), the distribution of phosphosite localization scores demonstrates that total number of phosphosites is still significantly lower with this MS^2 method, irrespective of search engine (Figure S4). Not surprisingly, site localization confidence generally decreased as the number of phosphorylation sites per peptide increased, irrespective of the search algorithm employed (Figures S5 and S6). The exception was EThcD OT: ∼76% of phosphosites were confidently localized with PTM-score independent of the number of phosphate groups; doubly phosphorylated peptides yielded a higher number of confidently localized phosphosites on average (93%) with *ptmRS* site than singly (86%) or triply (83%) phosphorylated peptides. The performance of Andromeda/PTM-score was uniformly weaker across all data sets compared with MASCOT/*ptmRS*. The exception was the EThcD IT data for singly phosphorylated peptides, where the percentage of confidently localized sites was more comparable for the two search algorithms (78% for Andromeda/PTM-score, 83% for MASCOT/*ptmRS*).

Although the trend in confident phosphosite identification is similar to that observed for the phosphopeptide library, the proportion of incorrect or ambiguous assignments is much higher in the lysate-derived peptides, possibly due the greater diversity of peptide size, and the true/false nature of the manner that the phosphopeptide library was used to define correct/incorrect site localization. In contrast, Andromeda/PTM-score performed much better than MASCOT/*ptmRS* with EThcD IT (but not EThcD OT) data, identifying 12.5% more phosphopeptides, and ∼7% more phosphosites with confidence (Table 3, Figure 2).

For both the HCD OT and HCD IT regimes where nl EThcD IT is triggered, the percentage of confidently assigned phosphosites increases with Andromeda/PTM-score compared with HCD alone, particularly for HCD IT. This reflects the high performance of Andromeda/PTM-score with EThcD IT data. However, the total numbers of phosphosites identified with HCD IT are much lower when neutral loss EThcD is triggered due to the increased time required for ETD. Interestingly, although 42% of HCD IT spectra contained precursor neutral loss product ions (either 98 or 80 amu, at ≥10% base peak signal), a significant number of these were not

DOI: 10.1021/acs.jproteome.7b00337
J. Proteome Res. 2017, 16, 3448−3459

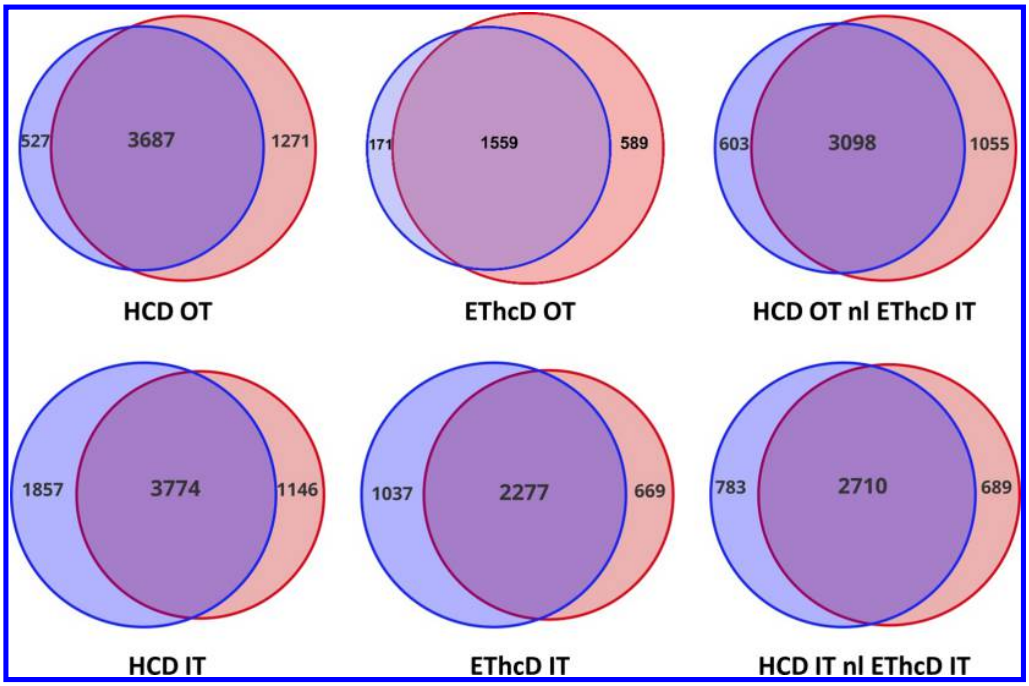

Figure 3. Overlap of phosphopeptide identification between search engines. Venn diagrams showing the number and overlap of phosphopeptides identified with either Andromeda/PTM-score (blue, left) or MASCOT/ptmRS (red, right) for each of the six MS acquisition methods applied to TiO_2-enriched U2OS cell lysate.

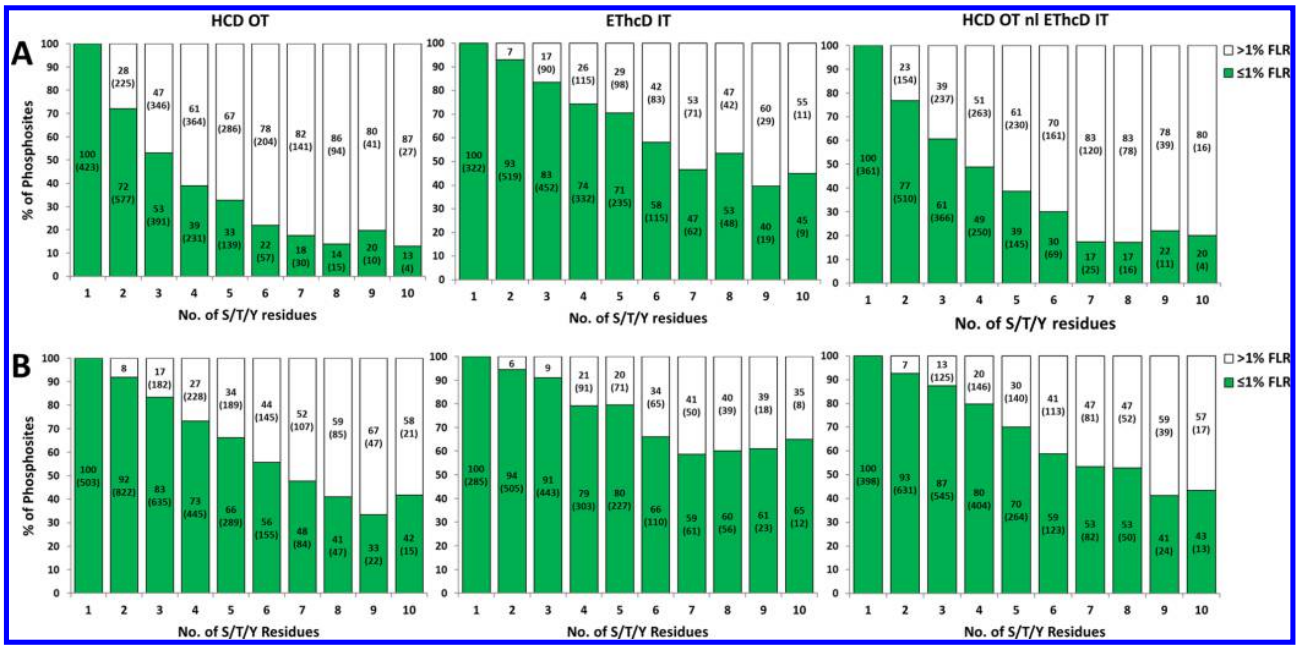

Figure 4. Number of confidently localized phosphosites as a function of the number of common putative phosphorylatable residues. Percent correctly site localized phosphopeptides (FLR ≤ 1%, green) or site ambiguous phosphopeptides (FLR > 1%, white) is presented as a function of the number of Ser (S), Thr (T), or Tyr (residues) within the peptide. Data generated by either HCD OT (left), EThcD IT (middle), or HCD nl EThcD OT (right) was search with either (A) Andromeda/PTM-score or (B) MASCOT/ptmRS as previously described. Percentage is indicated for each condition; the number of unique phosphosites is in parentheses. Data for all six MS acquisition methods are presented in Figures S7 and S8.

within the top 10 ions that triggered EThcD, and only 16% of HCD IT spectra precipitated the acquisition of EThcD.

The high proportion of confidently localized phosphosites with EThcD IT (76 and 83% from Andromeda/PTM-score and MASCOT/*ptmRS* respectively), combined with the fact that the two data analysis platforms yielded a high proportion of algorithm unique identifications (Figure 3), suggests that this mixed-mode fragmentation regime would likely benefit from data interrogation using multiple informatics pipelines: 31% of Andromeda/PTM-score identifications were unique, while 23% were unique to MASCOT/*ptmRS*. Perhaps not unexpectedly, the utility of EThcD OT for high-throughput phosphosite

DOI: 10.1021/acs.jproteome.7b00337
J. Proteome Res. 2017, 16, 3448−3459

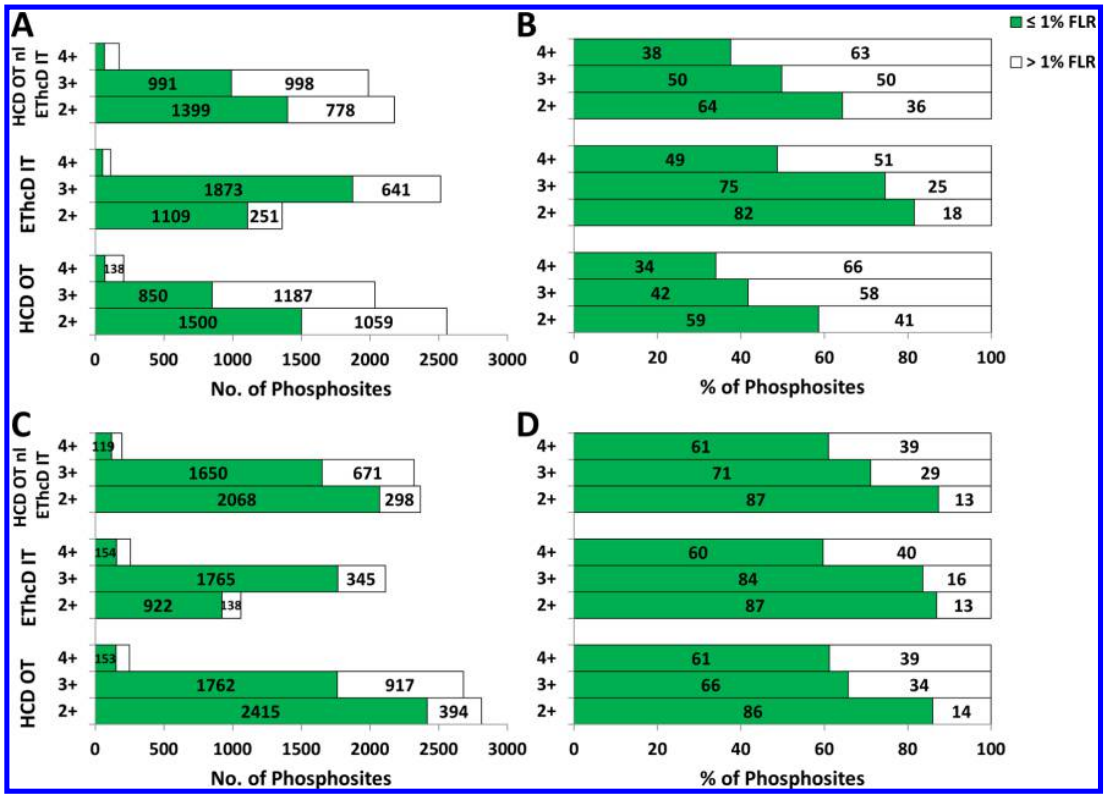

Figure 5. Phosphosite localization as a function of peptide ion charge state. Confidently localized phosphorylation sites (FLR ≤ 1%, green) or ambiguous phosphosite assignments (FLR > 1%, white) presented as a function of precursor ion charge state for data searched with Andromeda/PTM-score (A,B) or MASCOT/ptmRS (C,D). Number (A,C) or percentage (B,D) of phosphosites identified are indicated for each condition. Data for all six MS acquisition methods are presented in Figures S9 and S10.

identification was severely compromised due to the additional time required for both ETD and OT-based product ion analysis, resulting in much slower overall acquisition speeds for this high-resolution mixed mode fragmentation method. Consequently, there was a ~40−50% decrease in the number of confidently localized phosphosites using EThcD OT compared with HCD OT.

The difference in site localization confidence for HCD IT versus HCD OT data for the two algorithms becomes much more apparent for the complex cell-lysate-derived phosphopeptide sample compared with the synthetic phosphopeptide library, with site localization confidence decreasing from 76 to 60% for MASCOT/*ptmRS* and 50 to 37% for Andromeda/PTM-score (Figure 2B,D), again emphasizing the benefits of high-resolution MS^2 over the reduction in duty cycle afforded by analysis in the ion trap.

Evaluation of the distribution of site localization scores for all phosphopeptides facilitates a better understanding of how the two site localization algorithms handle the different fragmentation modes for this complex phosphopeptide sample (Figure S4). Scoring of EThcD IT data, particularly with *ptmRS*, yields a much shallower distribution of scores than those for HCD IT. Consequently, large changes in score result in relatively small changes in the number of confidently localized phosphosites. The distribution of scores for HCD OT data is notably distinct between the two algorithms. The elevated mass accuracy of the orbitrap allows *ptmRS* to maximize its ability to pinpoint the correct site of modification, with ~4000 phosphosites having a *ptmRS* score of 100. In contrast, PTM-score consistently scores low-resolution ion trap data higher, where the increased ion current and enhanced duty cycle likely yields benefits that are not compensated by the inability of this scoring system to handle high-resolution data.

Confident Phosphosite Localization Is Dependent on the Number of Potential Sites of Phosphorylation

To avoid potential confusion when examining the effect of multiple potential sites of phosphorylation (Ser, Thr, or Tyr) within a single peptide on site localization confidence, singly phosphorylated peptides only were considered for investigation (Figure 4; Figures S7 and S8). Unsurprisingly, as the number of Ser/Thr/Tyr residues increases, that is, the number of potential sites of modification increases, the numbers of confidently site localized phosphopeptides decreases with both *ptmRS* and PTM-score. For HCD OT-generated tandem mass spectra, this decrease in confident phosphosite localization is much more apparent with PTM-score than with *ptmRS*. For those phosphopeptides containing two Ser/Thr/Tyr residues, the phosphosite is confidently localized in 92% of cases using *ptmRS*, while only 72% are correctly localized with PTM-score. This decreases to 39% for PTM-score when a peptide contains four Ser/Thr/Tyr residues but only 73% for the same cohort when searched using *ptmRS*. The trend is consistent for HCD OT incorporating neutral-loss-triggered EThcD, with 80% of the peptides containing four Ser/Thr/Tyr residues from the *ptmRS* search having confident site localization but only 49% being confidently localized by PTM-score (Figure 4; Figures S7 and S8). For both scoring algorithms, the number of confidently assigned sites with HCD OT nl EThcD IT was

DOI: 10.1021/acs.jproteome.7b00337
J. Proteome Res. 2017, 16, 3448−3459

intermediary between the numbers observed with either HCD OT and EThcD IT, showing the potential benefit of the dual fragmentation approach when considering peptides with multiple possible sites of phosphorylation. Under all tandem MS conditions examined, MASCOT/ptmRS performed equal to or better than Andromeda/PTM-score for confident site localization, irrespective of the number putative sites of phosphorylation (Figure 4, Figures S7 and S8).

Effect of Charge State on Phosphosite Assignment

It is known that the efficiency of ETD is dependent on charge density and is thus optimal for tryptic peptides where the charge state is ≥3.[37] Given that EThcD is a dual fragmentation mechanism, generating both *b/y* (HCD) and *c/z* ions (ETD), the total number of ions generated using this fragmentation regime will thus be dependent on charge state, impacting the number of site-determining product ions. We therefore evaluated the effect of charge state on phosphosite localization confidence (Figure 5, Figures S9 and S10). Unsurprisingly, the ability to pinpoint the site of modification was notably improved with EThcD IT compared with HCD IT alone for precursor ions where z = 3, with either 84% (MASCOT/ptmRS) or 75% (Andromeda/PTM-score) of phosphosites being defined by EThcD compared with 53 or 29%, respectively, for HCD IT. The same is true for EThcD OT compared with HCD OT, with 77 or 42%, respectively, of 3+ peptide ions being correctly site localized with PTM score, cf. 87% (EThcD OT) and 66% (HCD OT) with *ptmRS* (Figures S9 and S10). EThcD IT also outperformed both HCD OT and HCD IT for confident site localization for ions of charge states 2+ and 4+, albeit with significantly fewer phosphosites being identified in total with EThCD IT than with either HCD method for 2+ ions (Figure 5, Figures S9 and S10).

Both of the MS acquisition strategies invoking EThcD as a consequence of precursor neutral loss (HCD IT nl EThcD; HCT OT nl EThcD) were compromised in terms of the efficiency and total number of phosphosites identified for 3+ and 4+ ions, with no apparent benefit.

CONCLUSIONS

In this investigation, we have systematically evaluated eight MS acquisition strategies on the Orbitrap Fusion mass spectrometer, a versatile tribrid MS platform, for their ability to confidently identify and, crucially, to pinpoint sites of modification on phosphopeptides. We have also examined the relative efficiency of two of the most widely used phosphoproteomics data analysis platforms for optimal phosphosite identification: MASCOT integrated into Proteome Discover using *ptmRS* and Andromeda with PTM-score.

Using a synthetic phosphopeptide library, we initially defined MS method-specific scores for Andromeda/PTM-score and MASCOT/*ptmRS* that yielded a 1% FLR. When applied to a complex biologically derived phosphopeptide mixture, even small changes in the applied scores may yield significant changes in the numbers of phosphosites identified for HCD-mediated fragmentation, and the marked difference in site confidence for the different MS methods at any given value cannot be ignored.

Our findings are largely in agreement with previous observations made using other orbitrap-based MS platforms, which demonstrate that phosphosite localization confidence is optimal with EThCD where a dual ion series is generated.[19] However, the total number of unique phosphopeptides identified, as well as the number of confidently localized phosphosites, is optimal when employing high-resolution analysis of HCD fragment ions for MS^2. MS acquisition strategies invoking neutral-loss-mediated ETD-based fragmentation are hampered by both the additional time taken to perform this type of fragmentation in a second round of MS^2 as well as the surprisingly few phosphopeptide ions that generate neutral loss product ions and thereby invoke this second round of MS^2 analysis.

Differences in the ways that the two bioinformatics platforms handle distinct types of tandem MS data and the number of unique phosphopeptides identified mean that there is likely to be a benefit in searching data acquired using a single acquisition strategy using both data analysis pipelines. This is particularly apparent with EThcD, where 31 and 23% of phosphopeptides, respectively are unique to either Andromeda/PTM-score or MASCOT/ptmRS. The relatively few unique phosphopeptide identifications with Andromeda for HCD OT data and the overall reduction in confident site localization using Andromeda/PTM-score for regimes exploiting fragmentation strategies other than EThcD mean that multialgorithm searching may not be of significant benefit with other types of data.

We conclude that optimal phosphoproteomics analysis on the Orbitrap Fusion Tribrid platform is achieved in the first instance using HCD OT and interrogation with MASCOT/ptmRS. Indeed, on the basis of the settings used and the amount of sample analyzed in these studies, we suggest that the benefits of acquiring high-resolution orbitrap data are largely negated when using Andromeda/PTM-score. Our data also highlight that there are likely to be additional benefits in terms of increased numbers of confidently localized phosphosites, by implementing EThcD for ions with charge state of ≥3+ and the employment of a multiple algorithm search strategy. Moreover, the "high-definition ETD" (ETD HD) permissible with the Orbitrap Fusion Lumos, which is reported to facilitate ETD on larger precursor ion populations, will likely result in even greater benefits when applied to such a charge-state-mediated data acquisition strategy for phosphoproteomics.

ASSOCIATED CONTENT

Supporting Information

The Supporting Information is available free of charge on the ACS Publications website at DOI: 10.1021/acs.jproteome.7b00337.

Table S1. Orbitrap Fusion Tribrid MS acquisition parameters for the eight methods assessed. Table S2. Evaluation of Andromeda score cutoff using synthetic phosphopeptides. Figure S1. Acquisition method-specific phosphosite localization. Figure S2. Overlap between technical replicates processed using Andromeda. Figure S3. Overlap between technical replicates processed using Mascot. Figure S4. Distribution of phosphosite localization scores for either PTM-score or ptmRS from cell lysate-derived phosphopeptides. Figure S5. Phosphosite localization confidence with Andromeda/PTM-score. Figure S6. Phosphosite localization confidence with MASCOT/ptmRS. Figure S7 Phosphosite localization confidence as determined using Andromeda/PTM-score as a function of prevalence of common putative phosphorylated residues. Figure S8. Phosphosite localization confidence as determined using MASCOT/ptmRS as a function of prevalence of common putative

DOI: 10.1021/acs.jproteome.7b00337
J. Proteome Res. 2017, 16, 3448−3459

phosphorylated residues. Figure S9. Phosphosite localization determined using Andromeda/PTM-score as a function of peptide ion charge state. Figure S10. Phosphosite localization determined using MASCOT/ptmRS as a function of peptide ion charge state. (PDF)

AUTHOR INFORMATION

Corresponding Author

*E-mail: Claire.Eyers@Liverpool.ac.uk. Tel: +44 151 795 4424.

ORCID

Patrick A. Eyers: 0000-0002-9220-2966

Claire E. Eyers: 0000-0002-3223-5926

Author Contributions

All authors have given approval to the final manuscript.

Notes

The authors declare no competing financial interest.

The mass spectrometry proteomics data have been deposited to the ProteomeXchange Consortium via the PRIDE partner repository with the dataset identifier PXD007058.

ACKNOWLEDGMENTS

We thank Dr. Jenny Ho (Thermo Scientific), Dr. Helen Flynn (The Francis Crick Institute) and members of the Centre for Proteome Research for helpful discussion, and Dr. Gopal Sapkota, University of Dundee for the U2OS T-Rex Flp-in cells. This work was supported in part by NorthWest Cancer Research (CR1088) and the Biotechnology and Biological Sciences Research Council (BBSRC; BB/L009501/1 to C.E.E. and BB/M025705/1 to A.R.J.). S.F. is supported by a BBSRC DTP Ph.D. studentship award.

ABBREVIATIONS

AGC, automatic gain control; CID, collision-induced dissociation; ETD, electron-transfer dissociation; ETcaD, electron transfer with supplemental collision activation; EThcD, electron-transfer higher energy collisional dissociation; HCD, higher energy collisional dissociation; PD, Proteome Discoverer; PTM, post-translational modification

REFERENCES

(1) Olsen, J. V.; Vermeulen, M.; Santamaria, A.; Kumar, C.; Miller, M. L.; Jensen, L. J.; Gnad, F.; Cox, J.; Jensen, T. S.; Nigg, E. A.; Brunak, S.; Mann, M. Quantitative phosphoproteomics reveals widespread full phosphorylation site occupancy during mitosis. *Sci. Signaling* **2010**, *3* (104), ra3.

(2) Koch, A.; Krug, K.; Pengelley, S.; Macek, B.; Hauf, S. Mitotic substrates of the kinase aurora with roles in chromatin regulation identified through quantitative phosphoproteomics of fission yeast. *Sci. Signaling* **2011**, *4* (179), rs6.

(3) Rigbolt, K. T.; Blagoev, B. Quantitative phosphoproteomics to characterize signaling networks. *Semin. Cell Dev. Biol.* **2012**, *23* (8), 863−71.

(4) Sun, Z.; Hamilton, K. L.; Reardon, K. F. Phosphoproteomics and molecular cardiology: techniques, applications and challenges. *J. Mol. Cell. Cardiol.* **2012**, *53* (3), 354−68.

(5) Umezawa, T.; Sugiyama, N.; Takahashi, F.; Anderson, J. C.; Ishihama, Y.; Peck, S. C.; Shinozaki, K. Genetics and phosphoproteomics reveal a protein phosphorylation network in the abscisic acid signaling pathway in Arabidopsis thaliana. *Sci. Signaling* **2013**, *6* (270), rs8.

(6) Li, J.; Silva-Sanchez, C.; Zhang, T.; Chen, S.; Li, H. Phosphoproteomics technologies and applications in plant biology research. *Front. Plant Sci.* **2015**, *6*, 430.

(7) Chan, C. Y.; Gritsenko, M. A.; Smith, R. D.; Qian, W. J. The current state of the art of quantitative phosphoproteomics and its applications to diabetes research. *Expert Rev. Proteomics* **2016**, *13* (4), 421−33.

(8) Noujaim, J.; Payne, L. S.; Judson, I.; Jones, R. L.; Huang, P. H. Phosphoproteomics in translational research: a sarcoma perspective. *Ann. Oncol* **2016**, *27* (5), 787−94.

(9) Swaffer, M. P.; Jones, A. W.; Flynn, H. R.; Snijders, A. P.; Nurse, P. CDK Substrate Phosphorylation and Ordering the Cell Cycle. *Cell* **2016**, *167* (7), 1750−1761.

(10) Gruber, W.; Scheidt, T.; Aberger, F.; Huber, C. G. Understanding cell signaling in cancer stem cells for targeted therapy - can phosphoproteomics help to reveal the secrets? *Cell Commun. Signaling* **2017**, *15* (1), 12.

(11) Kruse, R.; Hojlund, K. Mitochondrial phosphoproteomics of mammalian tissues. *Mitochondrion* **2017**, *33*, 45−57.

(12) Rabiee, A.; Schwammle, V.; Sidoli, S.; Dai, J.; Rogowska-Wrzesinska, A.; Mandrup, S.; Jensen, O. N. Nuclear phosphoproteome analysis of 3T3-L1 preadipocyte differentiation reveals system-wide phosphorylation of transcriptional regulators. *Proteomics* **2017**, *17* (6), 1600248.

(13) Bradshaw, R. A.; Burlingame, A. L.; Carr, S.; Aebersold, R. Reporting protein identification data: the next generation of guidelines. *Mol. Cell. Proteomics* **2006**, *5* (5), 787−8.

(14) Hsu, C. C.; Xue, L.; Arrington, J. V.; Wang, P.; Paez Paez, J. S.; Zhou, Y.; Zhu, J. K.; Tao, W. A. Estimating the Efficiency of Phosphopeptide Identification by Tandem Mass Spectrometry. *J. Am. Soc. Mass Spectrom.* **2017**, *28* (6), 1127−1135.

(15) Lanucara, F.; Lam, C.; Mann, J.; Monie, T. P.; Colombo, S. A.; Holman, S. W.; Boyd, J.; Dange, M. C.; Mann, D. A.; White, M. R.; Eyers, C. E. Dynamic phosphorylation of RelA on Ser42 and Ser45 in response to TNFalpha stimulation regulates DNA binding and transcription. *Open Biol.* **2016**, *6* (7), 160055.

(16) Lanucara, F.; Lee, D. C. H.; Eyers, C. E. Unblocking the sink: improved CID-based analysis of phosphorylated peptides by enzymatic removal of the basic C-terminal residue. *J. Am. Soc. Mass Spectrom.* **2014**, *25* (2), 214−25.

(17) Boersema, P. J.; Mohammed, S.; Heck, A. J. Phosphopeptide fragmentation and analysis by mass spectrometry. *J. Mass Spectrom.* **2009**, *44* (6), 861−78.

(18) Frese, C. K.; Altelaar, A. F.; van den Toorn, H.; Nolting, D.; Griep-Raming, J.; Heck, A. J.; Mohammed, S. Toward full peptide sequence coverage by dual fragmentation combining electron-transfer and higher-energy collision dissociation tandem mass spectrometry. *Anal. Chem.* **2012**, *84* (22), 9668−73.

(19) Frese, C. K.; Zhou, H.; Taus, T.; Altelaar, A. F.; Mechtler, K.; Heck, A. J.; Mohammed, S. Unambiguous phosphosite localization using electron-transfer/higher-energy collision dissociation (EThcD). *J. Proteome Res.* **2013**, *12* (3), 1520−5.

(20) Kim, M. S.; Zhong, J.; Kandasamy, K.; Delanghe, B.; Pandey, A. Systematic evaluation of alternating CID and ETD fragmentation for phosphorylated peptides. *Proteomics* **2011**, *11* (12), 2568−72.

(21) Hebert, A. S.; Richards, A. L.; Bailey, D. J.; Ulbrich, A.; Coughlin, E. E.; Westphall, M. S.; Coon, J. J. The one hour yeast proteome. *Mol. Cell. Proteomics* **2014**, *13* (1), 339−47.

(22) Espadas, G.; Borras, E.; Chiva, C.; Sabido, E. Evaluation of different peptide fragmentation types and mass analyzers in data-dependent methods using an Orbitrap Fusion Lumos Tribrid mass spectrometer. *Proteomics* **2017**, *17* (9), 1600416.

(23) Riley, N. M.; Mullen, C.; Weisbrod, C. R.; Sharma, S.; Senko, M. W.; Zabrouskov, V.; Westphall, M. S.; Syka, J. E.; Coon, J. J. Enhanced Dissociation of Intact Proteins with High Capacity Electron Transfer Dissociation. *J. Am. Soc. Mass Spectrom.* **2016**, *27* (3), 520−31.

(24) Olsen, J. V.; Macek, B.; Lange, O.; Makarov, A.; Horning, S.; Mann, M. Higher-energy C-trap dissociation for peptide modification analysis. *Nat. Methods* **2007**, *4* (9), 709−12.

DOI: 10.1021/acs.jproteome.7b00337
J. Proteome Res. 2017, 16, 3448−3459

(25) Zhang, Y.; Ficarro, S. B.; Li, S.; Marto, J. A. Optimized Orbitrap HCD for quantitative analysis of phosphopeptides. *J. Am. Soc. Mass Spectrom.* **2009**, *20* (8), 1425−34.
(26) Cui, L.; Yapici, I.; Borhan, B.; Reid, G. E. Quantification of competing H3PO4 versus HPO3 + H2O neutral losses from regioselective 18O-labeled phosphopeptides. *J. Am. Soc. Mass Spectrom.* **2014**, *25* (1), 141−8.
(27) Liu, F.; van Breukelen, B.; Heck, A. J. Facilitating protein disulfide mapping by a combination of pepsin digestion, electron transfer higher energy dissociation (EThcD), and a dedicated search algorithm SlinkS. *Mol. Cell. Proteomics* **2014**, *13* (10), 2776−86.
(28) Brunner, A. M.; Lossl, P.; Liu, F.; Huguet, R.; Mullen, C.; Yamashita, M.; Zabrouskov, V.; Makarov, A.; Altelaar, A. F.; Heck, A. J. Benchmarking multiple fragmentation methods on an orbitrap fusion for top-down phospho-proteoform characterization. *Anal. Chem.* **2015**, *87* (8), 4152−8.
(29) Bilan, V.; Leutert, M.; Nanni, P.; Panse, C.; Hottiger, M. O. Combining Higher-Energy Collision Dissociation and Electron-Transfer/Higher-Energy Collision Dissociation Fragmentation in a Product-Dependent Manner Confidently Assigns Proteomewide ADP-Ribose Acceptor Sites. *Anal. Chem.* **2017**, *89* (3), 1523−1530.
(30) Marx, H.; Lemeer, S.; Schliep, J. E.; Matheron, L.; Mohammed, S.; Cox, J.; Mann, M.; Heck, A. J.; Kuster, B. A large synthetic peptide and phosphopeptide reference library for mass spectrometry-based proteomics. *Nat. Biotechnol.* **2013**, *31* (6), 557−64.
(31) DeGnore, J. P.; Qin, J. Fragmentation of phosphopeptides in an ion trap mass spectrometer. *J. Am. Soc. Mass Spectrom.* **1998**, *9* (11), 1175−88.
(32) Wiese, H.; Kuhlmann, K.; Wiese, S.; Stoepel, N. S.; Pawlas, M.; Meyer, H. E.; Stephan, C.; Eisenacher, M.; Drepper, F.; Warscheid, B. Comparison of alternative MS/MS and bioinformatics approaches for confident phosphorylation site localization. *J. Proteome Res.* **2014**, *13* (2), 1128−37.
(33) Taus, T.; Kocher, T.; Pichler, P.; Paschke, C.; Schmidt, A.; Henrich, C.; Mechtler, K. Universal and confident phosphorylation site localization using phosphoRS. *J. Proteome Res.* **2011**, *10* (12), 5354−62.
(34) Olsen, J. V.; Blagoev, B.; Gnad, F.; Macek, B.; Kumar, C.; Mortensen, P.; Mann, M. Global, in vivo, and site-specific phosphorylation dynamics in signaling networks. *Cell* **2006**, *127* (3), 635−48.
(35) Cox, J.; Neuhauser, N.; Michalski, A.; Scheltema, R. A.; Olsen, J. V.; Mann, M. Andromeda: a peptide search engine integrated into the MaxQuant environment. *J. Proteome Res.* **2011**, *10* (4), 1794−805.
(36) Chalkley, R. J.; Clauser, K. R. Modification site localization scoring: strategies and performance. *Mol. Cell. Proteomics* **2012**, *11* (5), 3−14.
(37) Good, D. M.; Wirtala, M.; McAlister, G. C.; Coon, J. J. Performance characteristics of electron transfer dissociation mass spectrometry. *Mol. Cell. Proteomics* **2007**, *6* (11), 1942−51.

DOI: 10.1021/acs.jproteome.7b00337
J. Proteome Res. 2017, 16, 3448−3459